

Deeply virtual Compton scattering off Helium nuclei with positron beams

Sara Fucini¹, Mohammad Hattawy², Matteo Rinaldi¹, and Sergio Scopetta¹

¹ Dipartimento di Fisica e Geologia, Università degli studi di Perugia, and INFN, sezione di Perugia, via A. Pascoli snc, 06123, Perugia, Italy

² Old Dominion University, Norfolk, Virginia 23529, USA.

Received: date / Revised version: date

Abstract. Positron initiated deeply virtual Compton scattering (DVCS) off ^4He and ^3He nuclei is described. The way the so-called d -term could be obtained from the real part of the relevant Compton form factor is summarized, and the importance and novelty of this measurement is discussed. The measurements addressed for ^3He targets could be very useful even in a standard unpolarized target setup, measuring beam spin and beam charge asymmetries only. The unpolarized beam charge asymmetries for DVCS off ^3He and ^4He are also estimated, at JLab kinematics and, for ^4He , also at a configuration typical at the future Electron-Ion Collider. Incoherent DVCS processes, in particular the ones with tagging the internal target by measuring slow recoiling nuclei, and the unique possibility offered by positron beams for the investigation of Compton form factors of higher twist, are also briefly addressed.

PACS. 13.60.Hb, 14.20.Dh, 27.10.+h

Introduction

In recent years, a growing interest on nuclear deeply virtual Compton scattering (DVCS), i.e., hard photon electroproduction from nuclear targets, has arisen. This is mainly motivated by the possibility to shed light on the European Muon Collaboration (EMC) effect, i.e., the elusive nuclear modifications of the nucleon parton structure (see, e.g., Refs. [1,2] for recent reports), as well as the possibility to distinguish the so-called coherent and incoherent channels of the DVCS process. This latter feature has been experimentally recently achieved by the CLAS collaboration at JLab using a ^4He gaseous target [3,4,5], paving the way to a new class of precise measurements at high luminosity facilities. Coherent DVCS takes place when the nucleus recoils elastically, while in the incoherent process the struck proton is detected in the final state. Recently, the measurement of positron initiated DVCS has been experimentally proposed, in particular at JLab with the 12 GeV electron beam [6]. In the present paper, we analyze the impact that these measurements may have using ^4He and ^3He targets. This is done separately for the coherent and incoherent channels in the next two sections. Some additional remarks on higher twist effects are reported in the fourth section, followed by the conclusions of our investigation.

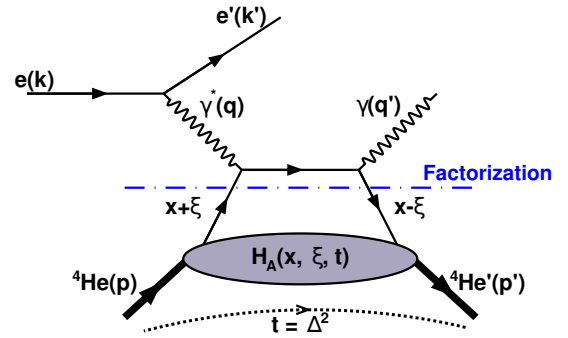


Fig. 1. The leading-order, twist-2, handbag approximation to the coherent DVCS process off ^4He , where the four-vectors of the initial/final electron, photon, and ^4He nucleus are denoted by k/k' , q/q' , and p/p' , respectively. The quantity $x + \xi$ is the hadron's longitudinal momentum fraction carried by the struck quark, -2ξ is the longitudinal momentum fraction of the momentum transfer Δ ($= q - q' = p' - p$), and t ($= \Delta^2$) is the squared momentum transfer.

Coherent DVCS

For the sake of concreteness, to explore the insights on how positron beams could help in this field, let us think first to coherent DVCS off ^4He , the only process which has been clearly accessed so far, illustrated, in the handbag approximation, in Fig. 1. In DVCS, the relevant non-perturbative

information is encoded in the so called generalized parton distribution functions (GPDs), giving access, in specific kinematic configurations, to the location, in the transverse plane of the target, of one parton of given longitudinal momentum (the so-called hadron tomography). We recall that ${}^4\text{He}$ has only one chiral-even GPD at leading-twist.

In the coherent DVCS data analysis from the EG6 experiment by the CLAS collaboration [3], the crucial measured observable was the single beam-spin asymmetry, A_{LU} , which can be extracted from the reaction yields with the two electron helicities (N^\pm):

$$A_{LU} = \frac{1}{P_B} \frac{N^+ - N^-}{N^+ + N^-}, \quad (1)$$

where P_B is the degree of longitudinal polarization of the incident electron beam.

Within the accessed kinematical phase-space of the EG6 experiment, the cross section of real photon electroproduction is dominated by the so-called Bethe-Heitler(BH) process, where the real photon is emitted by the incoming or the outgoing lepton, while the pure DVCS contribution is very small. However, the DVCS contribution is enhanced in the observables sensitive to the interference term, *i.e.* the quantity A_{LU} given above, which depends on the azimuthal angle ϕ between the (e, e') and $(\gamma^*, {}^4\text{He}')$ planes. The asymmetry A_{LU} for a spin-zero target can be approximated at leading-twist as

$$A_{LU}(\phi) = \frac{\alpha_0(\phi) \Im m(\mathcal{H}_A)}{\text{den}(\phi)}, \quad (2)$$

with:

$$\begin{aligned} \text{den}(\phi) = & \alpha_1(\phi) + \alpha_2(\phi) \Re e(\mathcal{H}_A) \\ & + \alpha_3(\phi) (\Re e(\mathcal{H}_A)^2 + \Im m(\mathcal{H}_A)^2). \end{aligned} \quad (3)$$

The kinematic factors α_i are known (see, e.g., Ref. [7,8]). In the experimental analysis, using the different contributions proportional to $\sin(\phi)$ and $\cos(\phi)$ in Eq. (3), both the real and imaginary parts of the so-called Compton Form Factor (CFF) \mathcal{H}_A , $\Re e(\mathcal{H}_A)$ and $\Im m(\mathcal{H}_A)$, respectively, have been extracted by fitting the $A_{LU}(\phi)$ distribution. Results of the impulse approximation calculation of Ref. [9], are shown together with the data of Ref. [3] in Figs. 2 and 3. In the theoretical calculation, use is made of state-of-the-art ingredients for the description of the nuclear and nucleon structure (older calculations are found in [10,11]). In particular, a convolution formula is obtained where the nuclear effects are governed by a model of a one-body non-diagonal spectral function based on the Av18 nucleon nucleon interaction [12] and the Urbana IX three body forces [13] (see Ref. [9] for details), while the nucleon GPDs are modelled following the Goloskokv-Kroll model [14,15,16]. Big statistical errors are seen everywhere in the data but, in particular, $\Re e(\mathcal{H}_A)$ is less precisely extracted than $\Im m(\mathcal{H}_A)$, due to the small coefficient α_2 in Eq. (3). This fact is easily understood looking at Fig. 3 where it is apparent that the predicted contribution of the real part of the CFF to the symmetry is really small.

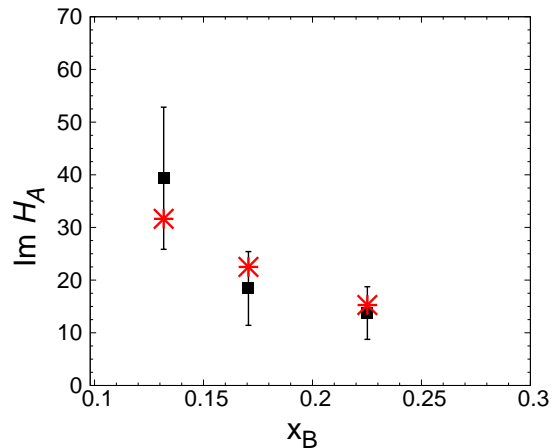


Fig. 2. The imaginary part of the CFF measured in coherent DVCS off ${}^4\text{He}$. Data from Ref. [3]; calculations (red crosses) from Ref. [9]

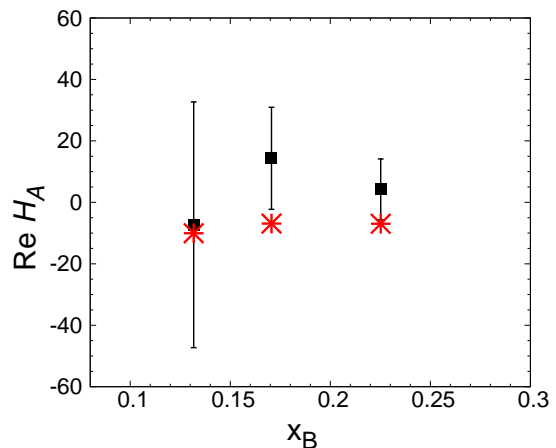


Fig. 3. The real part of the CFF measured in coherent DVCS off ${}^4\text{He}$. Data from Ref. [3]; calculations (red crosses) from Ref. [9].

Forth-coming data from JLab with 12 GeV electron beams at high luminosity, using also the detector system developed by the ALERT run-group [17], will be affected by much smaller statistical errors. Together with refined realistic theoretical calculations, in progress for light nuclei [18], the new data will help to unveil a possible exotic behavior of the real and imaginary part of \mathcal{H}_A , beyond that predicted in a conventional realistic scenario using the Impulse approximation. Nonetheless, the extracted $\Re e(\mathcal{H}_A)$ will be always less precise than $\Im m(\mathcal{H}_A)$, intrinsically, due to the small coefficient α_2 in (3) previously introduced. A precise knowledge of $\Re e(\mathcal{H}_A)$ for light nuclei would be instead crucial, as it is briefly analyzed in what follows, specified initially for the ${}^4\text{He}$ target. Formally one can write, for the quantities $\Re e(\mathcal{H}_A)$ and $\Im m\mathcal{H}_A$ shown

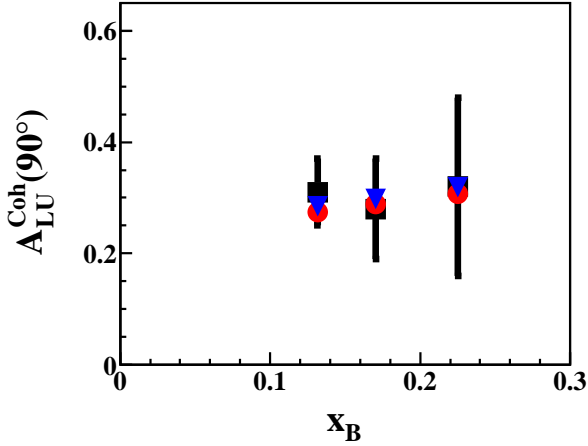


Fig. 4. The beam spin asymmetry measured in coherent DVCS off ${}^4\text{He}$, for $\phi = 90^\circ$. Data from Ref. [3]; calculations (red dots) from Ref. [9]. The result obtained neglecting the real part of the CFF \mathcal{H}_A is also shown (blue triangles)

in Figs. 3 and 2 respectively [19]:

$$\Re\mathcal{H}_A(\xi, t) \equiv \mathcal{P} \int_0^1 dx H_+(x, \xi, t) C_+(x, \xi), \quad (4)$$

and

$$\Im\mathcal{H}_A = -\pi H_+(\xi, \xi, t), \quad (5)$$

with:

$$H_+ = H(x, \xi, t) - H(-x, \xi, t), \quad (6)$$

and

$$C_+(x, \xi) = \frac{1}{x + \xi} + \frac{1}{x - \xi}, \quad (7)$$

with $H(x, \xi, t)$ the chiral-even, leading twist generalized parton distribution (GPD).

Besides, it is also known that $\Re(\mathcal{H}_A)$ satisfies a once subtracted dispersion relation at fixed t and can be therefore related to $\Im\mathcal{H}_A$, leading to [20, 21, 22, 23]

$$\Re\mathcal{H}_A(\xi, t) \equiv \mathcal{P} \int_0^1 dx H_+(x, x, t) C_+(x, \xi) - \delta(t). \quad (8)$$

One notices that, in contrast to the convolution integral defining the real part of the CFF in Eq. (4), where the GPD enters for unequal values of its first and second argument, the integrated in the dispersion relation corresponds to the GPD where its first and second arguments are equal. The subtraction term $\delta(t)$ can be related to the so-called d -term and accurate measurements, supplemented by precise calculations, would allow therefore to study this quantity for nuclei, for the first time. This d -term, introduced initially to recover the so-called

polynomiality property in double distribution (DD) approaches to GPDs modelling [24], has been related to the form factor of the QCD energy momentum tensor (see e.g. Ref. [25, 26]). It encodes information on the distribution of forces and pressure between elementary QCD degrees of freedom in the target. For nuclei, it has been predicted to behave as $A^{7/3}$ in a mean field scheme, either in the liquid drop model of nuclear structure [27] or in the Walecka model [28]. None of these approaches makes much sense for light nuclei, for which accurate realistic calculations are possible. Using light nuclei one would therefore explore, at the parton level, the onset and evolution of the mean field behavior across the periodic table, from deuteron to ${}^4\text{He}$, whose density and binding are not far from those of finite nuclei.

In this sense, coherent DVCS off ${}^3\text{He}$ targets acquire an important role: an intermediate behavior is expected between that of the almost unbound deuteron system and that of the deeply bound alpha particle. The formal description of coherent DVCS off ${}^3\text{He}$ follows that for the proton [7, 8], a spin one-half target, in terms of CFFs and related GPDs, accessed properly defining spin dependent asymmetries. Realistic theoretical calculations are available for GPDs [29, 30, 31, 32, 33] and are in progress for the relevant CFFs, cross sections and asymmetries, representing an important support to the planning of measurements [18]. We remark that in Refs. [31, 32] it has been shown that the ${}^3\text{He}$ chiral-even GPDs are strongly dominated by those of the neutron, which can be safely extracted by properly taking into account the nuclear effects described in the Impulse Approximation. One could object that the use of ${}^3\text{He}$, either longitudinally or transversely polarized, represents at the moment a challenge, either with electron or positron beams. Actually beam-charge asymmetries, built using electron and positron data, would represent, even with unpolarized ${}^3\text{He}$ targets and unpolarized beams, a possible access to $\Re\mathcal{H}_A(\xi, t)$, as previously described for ${}^4\text{He}$, with the same potential to explore the "d-" term for this relevant light nucleus.

Positron beams would guarantee this achievement: as a matter of fact, combining data for properly defined asymmetries measured using electrons and positrons, the role of $\Re\mathcal{H}_A$ would be directly accessed. Let us recall how it is possible.

One should notice that, between the quantities appearing in the above equations and the cross sections defining the generic photo- e^\pm production, in the following schematic general expression [6]:

$$\begin{aligned} \sigma_{\lambda 0}^e &= \sigma_{BH} + \sigma_{DVCS} + \lambda \tilde{\sigma}_{DVCS} \\ &+ e\sigma_{INT} + e\lambda \tilde{\sigma}_{INT}, \end{aligned} \quad (9)$$

the following relations hold:

$$\begin{aligned} \sigma_{BH} &\propto \alpha_1(\phi), \\ \sigma_{DVCS} &\propto \alpha_3(\phi) (\Re(\mathcal{H}_A)^2 + \Im\mathcal{H}_A^2), \\ \sigma_{INT} &\propto \alpha_2(\phi) \Re(\mathcal{H}_A), \\ \tilde{\sigma}_{INT} &\propto \alpha_0(\phi) \Im\mathcal{H}_A, \end{aligned} \quad (10)$$

while $\tilde{\sigma}_{DVCS}$ is proportional to a term kinematically suppressed at JLab kinematics, dependent on higher twist CFFs.

From a combined analysis of data taken with polarized electrons and/or positrons, one could access all the five cross sections in Eq. (9). We stress in particular that, using just unpolarized electrons and positrons, $\Re e(\mathcal{H}_A)$ would be directly accessed, building charge beam asymmetries. To expose this fact, in order to extract the real part of CFF, the beam charge asymmetry (BCA_A), for a nucleus with A nucleons, is introduced. By following the same formalism adopted in Ref. [7], one can define the BCA_A as follows:

$$\text{BCA}_A = \frac{d\sigma^+ - d\sigma^-}{d\sigma^+ + d\sigma^-}, \quad (11)$$

where here $d\sigma^\pm$ represents the five times differential unpolarized cross section for an electron (−) or a positron (+) beam, respectively. Let us recall that such a cross section for, e.g., the process $e^\pm \ ^3\text{He} \rightarrow e^\pm \ ^3\text{He}\gamma$ [7,8], reads:

$$d\sigma^C \equiv \frac{d\sigma^C}{dx_B dy dt d\phi d\varphi} = \frac{\alpha^3 x_B y}{16\pi^2 Q^2 \sqrt{1+\varepsilon^2}} \left| \frac{T_C}{e^3} \right|^2 \quad (12)$$

where $\varepsilon = 2x_B M_3/Q$, $C = \pm 1$ is the lepton charge, M_3 is the ^3He mass and y is the lepton energy fraction. Moreover ϕ is the azimuthal angle between the lepton plane and the recoiled nucleus. Finally, $T_C^2 = |T_{BH}|^2 + |T_{DVCS}|^2 + I_C$. Let us remark that only the interference term depends on the beam charge [7]. Therefore:

$$d\sigma^+ - d\sigma^- = \frac{2\alpha^3 x_B y}{16\pi^2 Q^2 \sqrt{1+\varepsilon^2}} \frac{I}{e^6} \quad (13)$$

where $I = I_C/C$. Within this formalism:

$$I = \frac{e^6}{x_B y^3 t P_1(\phi) P_2(\phi)} \times \left\{ c_0^I + \sum_1^3 [c_n^I \cos(n\phi) + s_n^I \sin(n\phi)] \right\}. \quad (14)$$

These harmonic coefficients depend on the ^3He CFFs. In particular, if unpolarized targets and beams are considered, s_n^I do not contribute to the BCA₃. The functions P_1 and P_2 [7] cancel out in the evaluation of BCA₃. On the other hand:

$$d\sigma^+ + d\sigma^- = \frac{2\alpha^3 x_B y}{16\pi^2 Q^2 \sqrt{1+\varepsilon^2}} \frac{|T_{DVCS}|^2 + |T_{BH}|^2}{e^3}. \quad (15)$$

We remind that, when terms of the order t/Q^2 can be neglected, BCA₃ is directly related to the real part of CFFs. As a matter of facts, in this kinematic conditions,

$$\text{BCA}_3(\phi) \sim \frac{e^6}{x_B y^3 \Delta^2 P_1(\phi) P_2(\phi)} \frac{c_1^I \cos(\phi)}{|T_{BH}|^2}. \quad (16)$$

We remind that, since c_3^I is related to the gluon distribution, in this initial analysis such a contribution is also neglected, together with c_0^I and c_2^I . Finally $c_1^I \propto \text{Re } c_{unp}^I$ where $c_{unp}^I = F_1 \mathcal{H} + x_B/(2-x_B)(F_1+F_2)\tilde{\mathcal{H}} - \Delta^2/(4M^2)F_2 \mathcal{E}$ (for details see Ref. [7]). We recall that F_1 and F_2 are the Dirac and Pauli form factors respectively and $\mathcal{F} = \mathcal{H}, \mathcal{E}, \tilde{\mathcal{H}}$ is the CFF. Finally:

$$\text{BCA}_3(\phi) = \frac{x_B(1+\varepsilon^2)^2}{y} \frac{c_1^I \cos(\phi)}{c_0^{BH} + c_1^{BH} \cos(\phi)}. \quad (17)$$

Numerical predictions for the ^3He BCA, evaluated in a kinematical range typical at JLab, are shown for the first time in the upper panel of Fig. 5. Here the ^3He GPDs have been calculated by following the line of Refs. [31,32], i.e. by means of the off-forward spin dependent spectral function calculated from the ^3He wave function corresponding to the AV18 nuclear potential [34,35,36]. The nucleonic GPDs, necessary as an input to the calculations, have been chosen among the phenomenological parametrizations of Refs. [14,15,16]. In addition one can introduce the nuclear beam spin asymmetry (BSA):

$$\text{BSA}_A = \frac{d\sigma^\uparrow - d\sigma^\downarrow}{d\sigma^\uparrow + d\sigma^\downarrow}. \quad (18)$$

By using the previously discussed strategy and approximations, one can relate the above quantity to the imaginary part of CFF. For a 1/2 spin target like the ^3He one gets:

$$\text{BSA}_3 \sim \pm \frac{x_{Bj}}{y} \frac{s_1^I}{c_0^{BH}} \sin(\phi), \quad (19)$$

where now $s_1^I \propto \text{Im } c_{unp}^I$.

The formalism above discussed for the beam charge asymmetry of the ^3He nucleus can be easily extended to the ^4He nucleus. While the beam spin asymmetry for a longitudinally polarized electron beam off an unpolarized target has already demonstrated to be a key observable to access the imaginary part of the CFF, the BCA is mostly useful to extract information for the real part Eq. (8). Looking at Eq. (17), the numerator cleanly encapsulates the real part of CFF linked to the chiral even GPD of the H_q^A . Conversely to the ^3He case, the ^4He spinless nature allows one the access to only this GPDs without the contamination of other GPDs. We show here our first estimates of the BCA for ^4He . We make use, for the expression of the GPD H_q^A of the impulse approximation model presented in Ref. [9] where, as already reported, a semi-realistic model for the nuclear part, accounting for a realistic momentum dependence obtained with realistic NN potential (Av18) and three-body forces, was adopted.

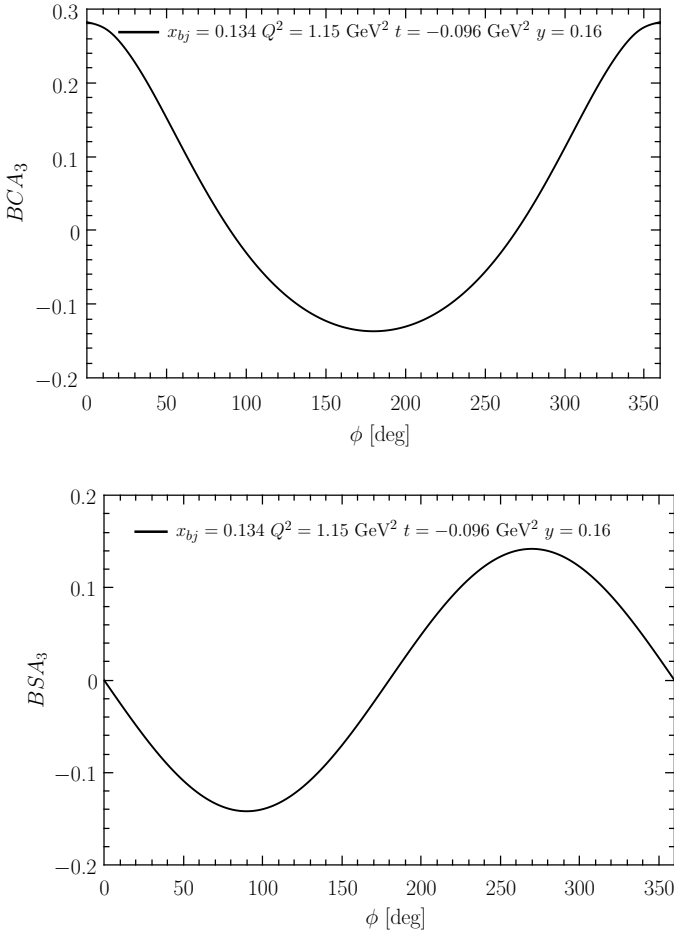


Fig. 5. Upper panel: The ${}^3\text{He}$ beam charge asymmetry Eq. (17) for a specific kinematic configuration, typical at JLab. Lower panel: the same but for the ${}^3\text{He}$ beam spin asymmetry Eq. (19).

While the non diagonal momentum and the energy dependencies of the spectral function is just modeled, a confirmation of the capability of our model to describe conventional nuclear effects is at hand. As an example of this fact, one can check Figs. 2-3. In passing by, we remind that the twist-two CFF of the ${}^4\text{He}$ nucleus receives the contribution of the GPD H and E of the bound nucleons in the form $H_q^{N/A} = \sqrt{(1 - \xi^2)} \left[H_q^N - \frac{\xi^2}{1 - \xi^2} E_q^N \right]$. As noted in Ref. [18], the contribution of the GPD E_q^N is practically negligible at the kinematics probed at JLab due to the smallness of the skewness (an even greater kinematical suppression for such a factor will be observed in the typical kinematic ranges expected at the Electron Ion Collider (EIC) [37]). For the GPDs of the nucleons, we made use of the same GK models used for ${}^3\text{He}$, i.e. the ones described in Refs. [38, 15]. In Fig. 7, a sizable asymmetry is observed for ${}^4\text{He}$ plotted at various kinematics. Two of these are the same already probed in Ref. [3], while another one is the same foreseen for the free proton using positron beams (see. Ref. [39]). As a reference, we show in Fig. 6 the same quantity

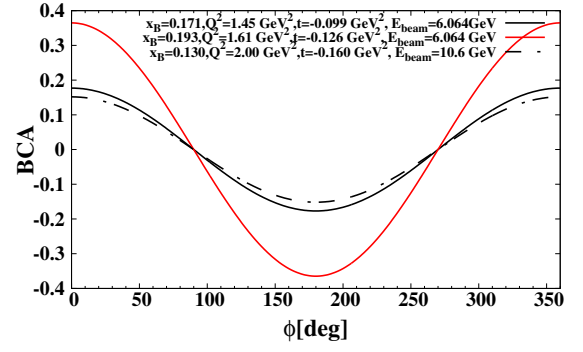


Fig. 6. The ${}^4\text{He}$ beam charge asymmetry shown at different kinematic points, typical at JLab.

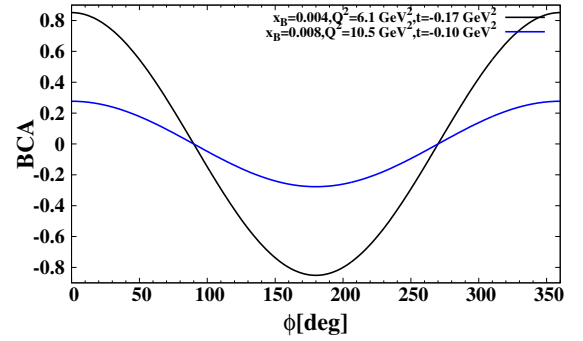


Fig. 7. The ${}^4\text{He}$ beam charge asymmetry shown at different EIC kinematics. The energy configuration corresponding to these plots is $E_{\text{electron}} \times E_{\text{nucleus}} = (18 \times 110)$ GeV.

for one of the kinematic points envisioned at the EIC for a positron beam at 18 GeV colliding with an helium-4 beam with an energy of 110 GeV. The kinematic points plotted in the present paper have been obtained as pseudo-data generated with the software TOPEG.

While in Ref. [37] the possibility to reach the first tomographic view of the nucleus is shown, here the big asymmetry found in some of the kinematical ranges investigated, allowing one an easier extraction of information from the observable, confirms the prominent role that the EIC together with the upgraded JLab will play with the aim to reach a deeper comprehension of the innermost structure of hadronic targets and hadronic matter.

Incoherent DVCS

A subject aside is represented by incoherent DVCS off He nuclei, i.e., the process where, in the final state, the struck proton is detected, its CFFs accessed, its GPDs, in principle, extracted and, ultimately, its tomography obtained. Fig. 8 illustrates the leading-twist handbag diagram for the incoherent DVCS process off ${}^4\text{He}$. Such measurements would provide a pictorial representation of the realization

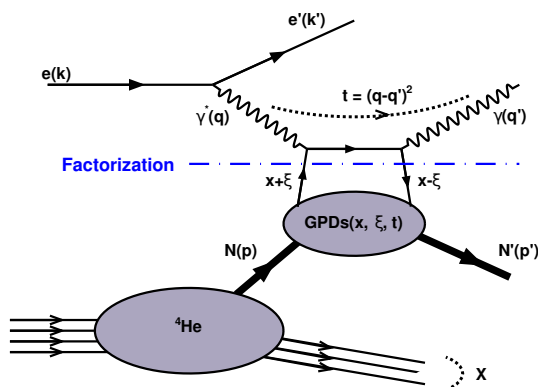


Fig. 8. The leading-order, twist-2, handbag approximation to incoherent DVCS off ${}^4\text{He}$. See Fig. 1 for the definition of the variables.

of the EMC effect and a great progress towards the understanding of its dynamical origin. As already stressed, this channel has been successfully isolated by the EG6 experiment of the CLAS collaboration at JLab [4] and a first glimpse at the parton structure of the bound proton in the transverse coordinate space is therefore at hand. Recent impulse approximation calculations, using again a description based on the Av18 interaction for the nuclear effects and, for the nucleon part, the GK model and the one proposed in Ref [40], evaluated using the PARTON tool [41], have been presented in Refs [42,43]. The theoretical description of the recent data with conventional realistic ingredients is rather encouraging. The program at JLab 12 includes an improvement of the accuracy of these measurements, in particular, for the first time in DVCS, tagging the struck nucleon detecting slow recoiling nuclei, using the detector developed by the ALERT run group [44]. This would allow to keep possible final state interactions, relevant in principle in this channel, under control. Measurements performed with electron and positron beams would allow for example the measurement of the d -term for the bound nucleon, either proton in ${}^3\text{He}$ (tagging 2H from DVCS on ${}^3\text{He}$) or in ${}^4\text{He}$ (tagging ${}^3\text{H}$ from DVCS on ${}^4\text{He}$) or neutron in ${}^4\text{He}$ (tagging ${}^3\text{He}$ from DVCS on ${}^4\text{He}$). Modifications of the d -term of the nucleon in the nuclear medium, studied e.g. in Ref. [28], would be at hand, as well as a glimpse at the structure of the neutron in the transverse plane, complementary to that obtained with deuteron targets.

Beyond a chiral even GPDs description of DVCS on ${}^4\text{He}$

As a last argument, we quickly note that, from the measurement of beam spin asymmetries built using cross sections measured with polarized electrons and positrons in coherent DVCS off ${}^4\text{He}$, the terms $\tilde{\sigma}_{DVCS}$ and $\tilde{\sigma}_{INT}$, appearing in Eq. 9, could be independently accessed. This

would allow, for example for ${}^4\text{He}$, to study the other leading twist CFF of a spinless target, the so called gluon transversity GPD H_T , giving a corresponding name to the CFF \mathcal{H}_T , appearing in $\tilde{\sigma}_{DVCS}$. In Ref. [8], it is shown how the contribution of \mathcal{H}_T to the cross section occurs through an interference between twist-two and effective twist-three CFFs. A first glimpse at this complicated interrelation would be obtained for a spin-less target, in particular for a nuclear target, for the first time. As for any other gluon-sensitive observable, data for the cross section $\tilde{\sigma}_{DVCS}$ would be a perfect tool to study gluon dynamics in nuclei. For example, a comparison between the above observable and calculations performed in an Impulse Approximation scheme, where the relevant nuclear degrees of freedom are colorless nucleons and mesons, would have the potential to expose possible exotic gluon dynamics in nuclei. This would be a pretty new possibility, complementary to that planned at JLab with 12 GeV, using exclusive vector meson electroproduction off ${}^4\text{He}$ [44]. Such an interesting behavior would be very hardly seen using electrons only, due to the strong kinematical suppression of $\tilde{\sigma}_{DVCS}$ with respect to the other contributions in Eq. (9).

Conclusions

The unique possibilities offered by the use of positron beams in DVCS off three- and four-body nuclear systems have been reviewed. Summarizing, we can conclude that the main advantages will be:

- in coherent DVCS off ${}^3\text{He}$ and ${}^4\text{He}$, using polarized electrons and unpolarized positrons, the real part of the chiral even unpolarized CFFs would be measured with a precision comparable to that of their imaginary part, providing a tool for the study of the so called d -term. In turn, the distribution of pressure and forces between the partons in nuclei, a new way to look at the nuclear medium modifications of nucleon structure, could be investigated;
- in incoherent DVCS off ${}^3\text{He}$ and ${}^4\text{He}$, possibly tagging slow recoiling nuclear systems, the same programme could be run for the bound proton and neutron;
- using polarized ${}^3\text{He}$ targets, a more complicated setup for the moment, spin dependent and parton helicity flip CFFs would be accessed for the first time for a nucleus, in both their real and imaginary parts. Moreover, in this case these quantities would be dominated by the neutron contributions and, in turn, an extraction of the neutron CFFs would be feasible;
- coherent DVCS off ${}^4\text{He}$, initiated with polarized positrons, would allow a first analysis of nuclear chiral odd CFFs and GPDs, with higher twist contamination suitable to tentatively explore gluon dynamics in nuclei.

A programme of nuclear measurements with positron beams would represent therefore an exciting complement to the experiments planned with nucleon targets, and to those planned with nuclear targets and electron beams. In this paper, we have shown for the first time realistic

Impulse Approximation predictions for spin-independent charge asymmetries, at JLab kinematics for ^3He and ^4He and, in this last case, also in one of the typical kinematic setups foreseen at the EIC. In an extended forthcoming investigation these calculations will be extended to the incoherent channels and to other spin dependent asymmetries.

References

1. R. Dupré and S. Scopetta. 3D Structure and Nuclear Targets. *Eur. Phys. J.*, A52(6):159, 2016.
2. I. C. Cloët et al. Exposing Novel Quark and Gluon Effects in Nuclei. *J. Phys.*, G46(9):093001, 2019.
3. M. Hattawy et al. First Exclusive Measurement of Deeply Virtual Compton Scattering off ^4He : Toward the 3D Tomography of Nuclei. *Phys. Rev. Lett.*, 119(20):202004, 2017.
4. M. Hattawy et al. Exploring the Structure of the Bound Proton with Deeply Virtual Compton Scattering. *Phys. Rev. Lett.*, 123(3):032502, 2019.
5. R. Dupré et al. Measurement of deeply virtual Compton scattering off Helium-4 with CLAS at Jefferson Lab, 2102.07419/nucl-ex. 2 2021.
6. A. Accardi et al. e^+ @JLab White Paper: An Experimental Program with Positron Beams at Jefferson Lab, arxiv:2007.15081/nucl-ex.
7. Andrei V. Belitsky, Dieter Mueller, and A. Kirchner. Theory of deeply virtual Compton scattering on the nucleon. *Nucl. Phys.*, B629:323–392, 2002.
8. Andrei V. Belitsky and Dieter Mueller. Refined analysis of photon leptonproduction off spinless target. *Phys. Rev.*, D79:014017, 2009.
9. Sara Fucini, Sergio Scopetta, and Michele Viviani. Coherent deeply virtual Compton scattering off ^4He . *Phys. Rev.*, C98(1):015203, 2018.
10. S. Liuti and S.K. Taneja. Microscopic description of deeply virtual Compton scattering off spin-0 nuclei. *Phys. Rev. C*, 72:032201, 2005.
11. V. Guzey and M. Strikman. DVCS on spinless nuclear targets in impulse approximation. *Phys. Rev. C*, 68:015204, 2003.
12. Robert B. Wiringa, V. G. J. Stoks, and R. Schiavilla. An Accurate nucleon-nucleon potential with charge independence breaking. *Phys. Rev. C*, 51:38–51, 1995.
13. B. S. Pudliner, V. R. Pandharipande, J. Carlson, Steven C. Pieper, and Robert B. Wiringa. Quantum Monte Carlo calculations of nuclei with $A \leq 7$. *Phys. Rev. C*, 56:1720–1750, 1997.
14. Peter Kroll, Herve Moutarde, and Franck Sabatie. From hard exclusive meson electroproduction to deeply virtual Compton scattering. *Eur. Phys. J.*, C73(1):2278, 2013.
15. S. V. Goloskokov and P. Kroll. The Target asymmetry in hard vector-meson electroproduction and parton angular momenta. *Eur. Phys. J.*, C59:809–819, 2009.
16. Markus Diehl and Peter Kroll. Nucleon form factors, generalized parton distributions and quark angular momentum. *Eur. Phys. J.*, C73(4):2397, 2013.
17. Whitney Armstrong et al. Partonic Structure of Light Nuclei, arxiv:1708.00888/nucl-ex. 2017.
18. Sara Fucini, Matteo Rinaldi, and Sergio Scopetta. Generalized parton distributions of light nuclei. *Few Body Syst.*, 62(1):3, 2021.
19. Michel Guidal, Hervé Moutarde, and Marc Vanderhaeghen. Generalized Parton Distributions in the valence region from Deeply Virtual Compton Scattering. *Rept. Prog. Phys.*, 76:066202, 2013.
20. I. V. Anikin and O. V. Teryaev. Dispersion relations and subtractions in hard exclusive processes. *Phys. Rev.*, D76:056007, 2007.

21. M. Diehl and D. Yu. Ivanov. Dispersion representations for hard exclusive processes: beyond the Born approximation. *Eur. Phys. J.*, C52:919–932, 2007.
22. A. V. Radyushkin. Generalized Parton Distributions and Their Singularities. *Phys. Rev.*, D83:076006, 2011.
23. B. Pasquini, M. V. Polyakov, and M. Vanderhaeghen. Dispersive evaluation of the D-term form factor in deeply virtual Compton scattering. *Phys. Lett.*, B739:133–138, 2014.
24. Maxim V. Polyakov and C. Weiss. Skewed and double distributions in pion and nucleon. *Phys. Rev.*, D60:114017, 1999.
25. Maxim V. Polyakov and Peter Schweitzer. Forces inside hadrons: pressure, surface tension, mechanical radius, and all that. *Int. J. Mod. Phys.*, A33(26):1830025, 2018.
26. H. Dutrieux, C. Lorcé, H. Moutarde, P. Sznajder, A. Trawiński, and J. Wagner. Phenomenological assessment of proton mechanical properties from deeply virtual Compton scattering. *Eur. Phys. J. C*, 81(4):300, 2021.
27. M. V. Polyakov. Generalized parton distributions and strong forces inside nucleons and nuclei. *Phys. Lett.*, B555:57–62, 2003.
28. Ju-Hyun Jung, Ulugbek Yakhshiev, Hyun-Chul Kim, and Peter Schweitzer. In-medium modified energy-momentum tensor form factors of the nucleon within the framework of a π - ρ - ω soliton model. *Phys. Rev.*, D89(11):114021, 2014.
29. Sergio Scopetta. Generalized parton distributions of He-3. *Phys. Rev.*, C70:015205, 2004.
30. S. Scopetta. Conventional nuclear effects on generalized parton distributions of trinucleons. *Phys. Rev.*, C79:025207, 2009.
31. M. Rinaldi and S. Scopetta. Extracting generalized neutron parton distributions from ^3He data. *Phys. Rev.*, C87(3):035208, 2013.
32. M. Rinaldi and S. Scopetta. Neutron orbital structure from generalized parton distributions of ^3He . *Phys. Rev.*, C85:062201, 2012.
33. Matteo Rinaldi and Sergio Scopetta. Theoretical description of deeply virtual Compton scattering off ^3He . *Few Body Syst.*, 55:861–864, 2014.
34. E. Pace, G. Salme, S. Scopetta, and A. Kievsky. Neutron structure function $F_2^{*n}(x)$ from deep inelastic electron scattering off few nucleon systems. *Phys. Rev.*, C64:055203, 2001.
35. A. Kievsky, E. Pace, G. Salme, and M. Viviani. Neutron electromagnetic form-factors and inclusive scattering of polarized electrons by polarized He-3 and He-3 targets. *Phys. Rev.*, C56:64–75, 1997.
36. A. Kievsky, M. Viviani, and S. Rosati. Study of bound and scattering states of three nucleon systems. *Nucl. Phys.*, A577:511–527, 1994.
37. R. Abdul Khalek et al. Science Requirements and Detector Concepts for the Electron-Ion Collider: EIC Yellow Report, 2103.05419/physics.ins-det. 3 2021.
38. S.V. Goloskokov and P. Kroll. The Longitudinal cross-section of vector meson electroproduction. *Eur. Phys. J. C*, 50:829–842, 2007.
39. V. Burkert et al. Beam charge asymmetries for deeply virtual Compton scattering off the proton, 2103.12651/nuclex. 3 2021.
40. C. Mezrag, H. Moutarde, and F. Sabatié. Test of two new parametrizations of the generalized parton distribution H. *Phys. Rev. D*, 88(1):014001, 2013.
41. B. Berthou et al. PARTONS: PARTonic Tomography Of Nucleon Software: A computing framework for the phenomenology of Generalized Parton Distributions. *Eur. Phys. J. C*, 78(6):478, 2018.
42. Sara Fucini, Sergio Scopetta, and Michele Viviani. Catching a glimpse of the parton structure of the bound proton. *Phys. Rev.*, D101(7):071501, 2020.
43. Sara Fucini, Sergio Scopetta, and Michele Viviani. Incoherent deeply virtual Compton scattering off ^4He . *Phys. Rev. C*, 102:065205, 2020.
44. Whitney R. Armstrong et al. Spectator-Tagged Deeply Virtual Compton Scattering on Light Nuclei, arxiv:1708.00835/nuclex. 2017.